Electronic Supplementary Material (ESI) for ChemComm.

Controlling the quantity of γ-Fe inside multiwall carbon nano-onions: the key role of sulfur

Supplementary section

Jiaxin Song[a+], Xilong Guo[a+], Lin Zhang[a+], Omololu Odunmbaku[b], Hansong Wu[a], Shanling Wang[c], Jiqiu Wen[c], Aiqun Gu[c], Jian Guo[a], Hong Zhang[a]* and Filippo S.Boi[a]*

a. College of Physics, Sichuan University, Chengdu, China

b. MOE Key Laboratory of Low-grade Energy Utilization Technologies and Systems, CQU-NUS Renewable Energy Materials & Devices Joint Laboratory, School of Energy and Power Engineering, Chongqing University, Chongqing 400044, China.

c. Analytical and Testing Center, Sichuan University, Chengdu, China

+ = equally first authors

Corresponding author: f.boi@scu.edu.cn, hongzhang@scu.edu.cn

Supplementary Data on filled CNOs (produced with a progressive enhancement of sulfur quantity)

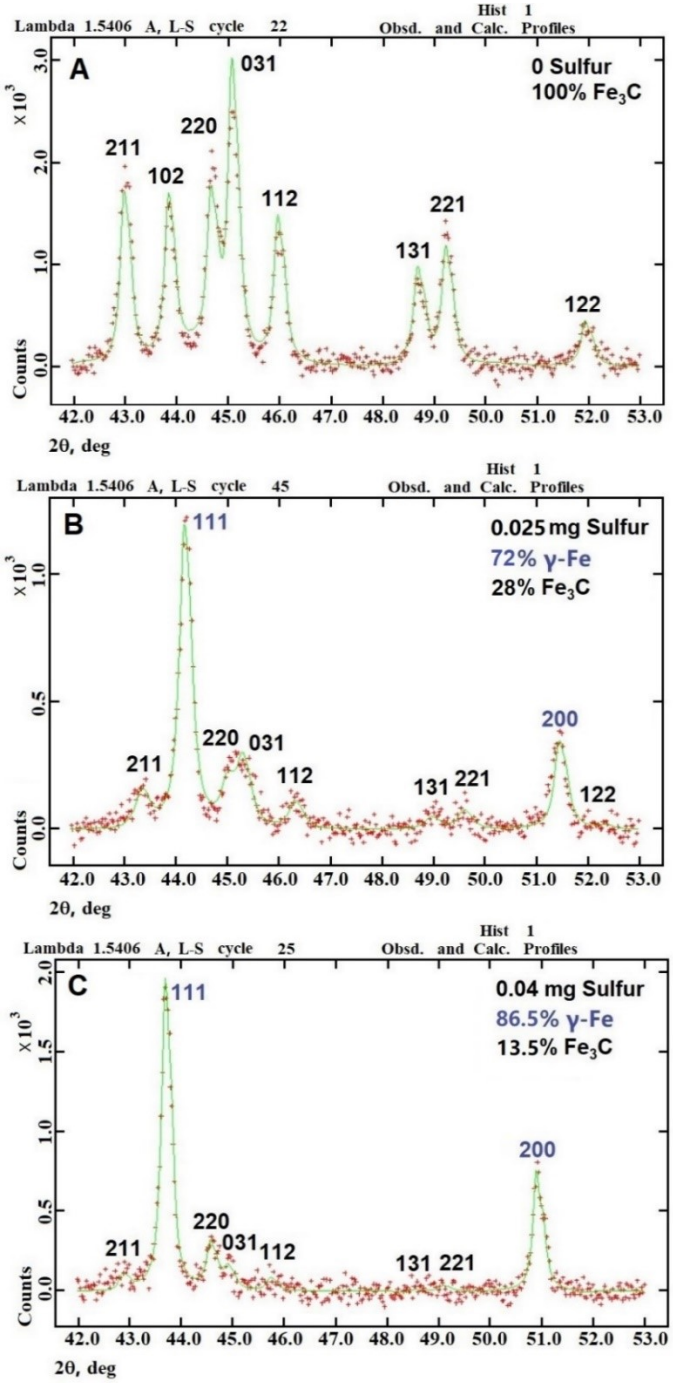

Figure S1: Rietveld refinement analyses of the diffractograms acquired from the samples obtained with a progressive introduction of sulfur in the CVS experiment. We highlight a progressive enhancement in the relative abundance of γ-Fe as the quantity of sulfur was increased to 0.04 mg, with a transition from a CNT-morphology (without sulfur) to a CNO-morphology in presence of sulfur.

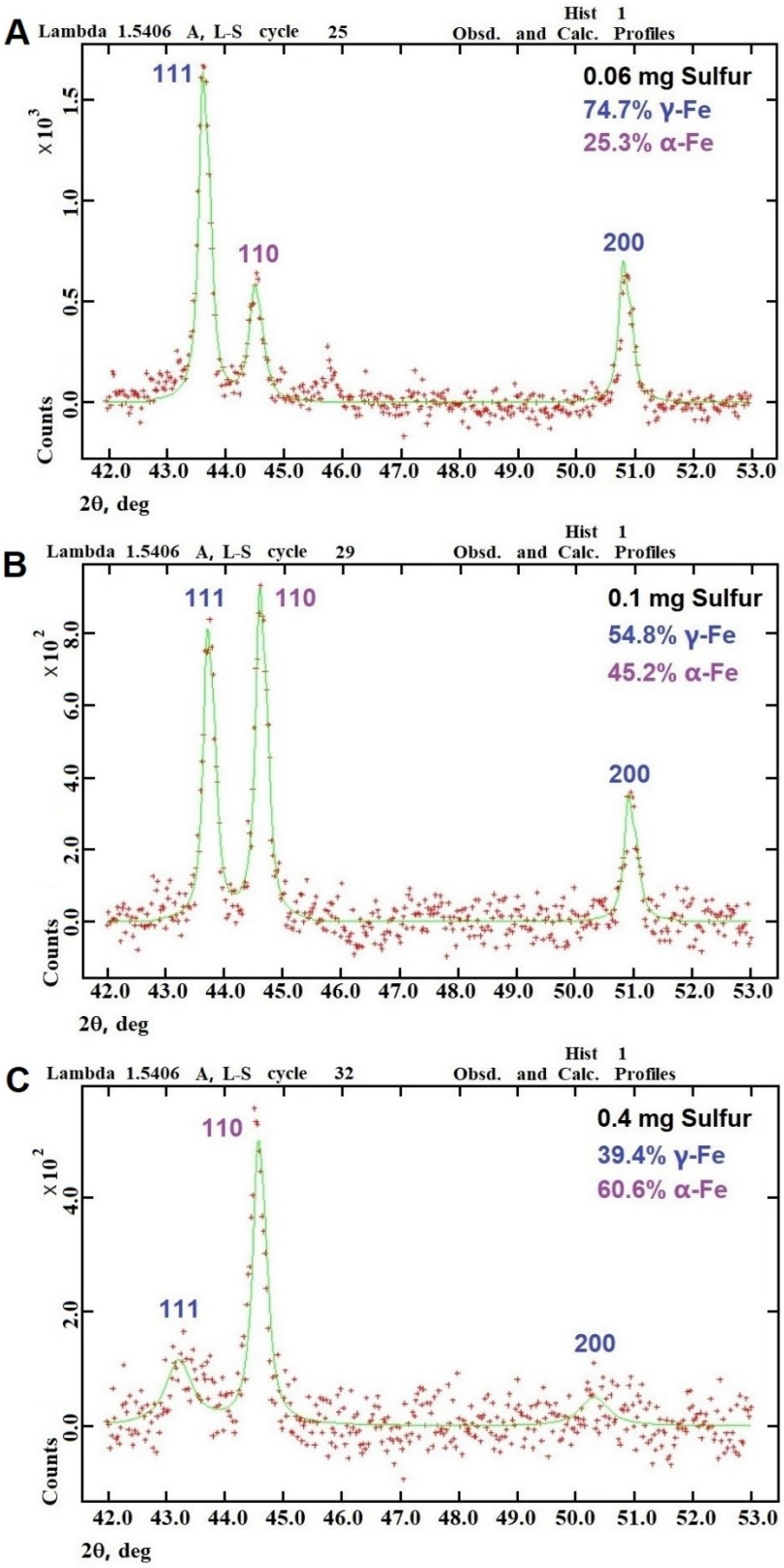

Figure S2: In A-C, additional Rietveld refinement analyses of the diffractograms acquired from CNOs filled with a controlled quantity of γ-Fe. A progressive depletion in the relative abundance of γ-Fe is found for quantity of sulfur larger than 0.04 mg.

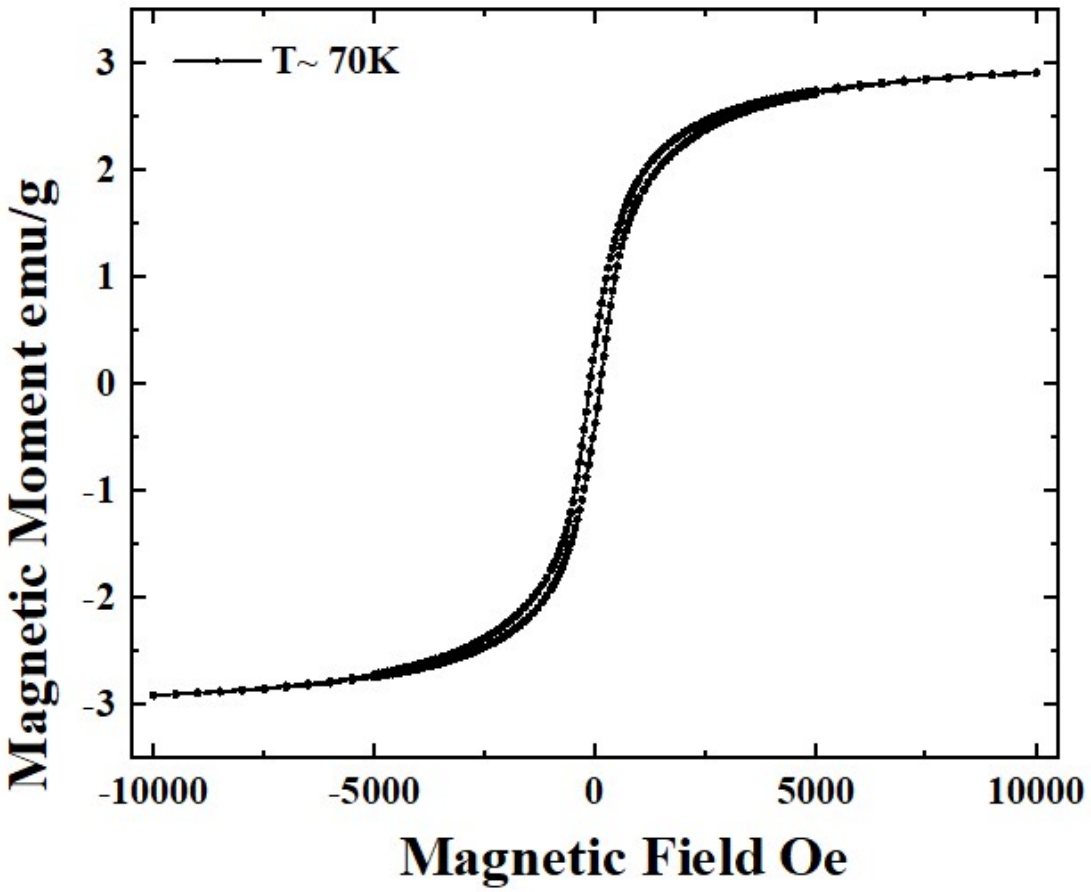

Figure S3: Magnetization hysteresis acquired at T~70K with maximum field of 10000 Oe from a CNO-sample encapsulating 80% of γ-Fe and 20% of Fe_3C.

Supplementary Data on filled CNTs (comparative analyses, samples produced in absence of sulfur)

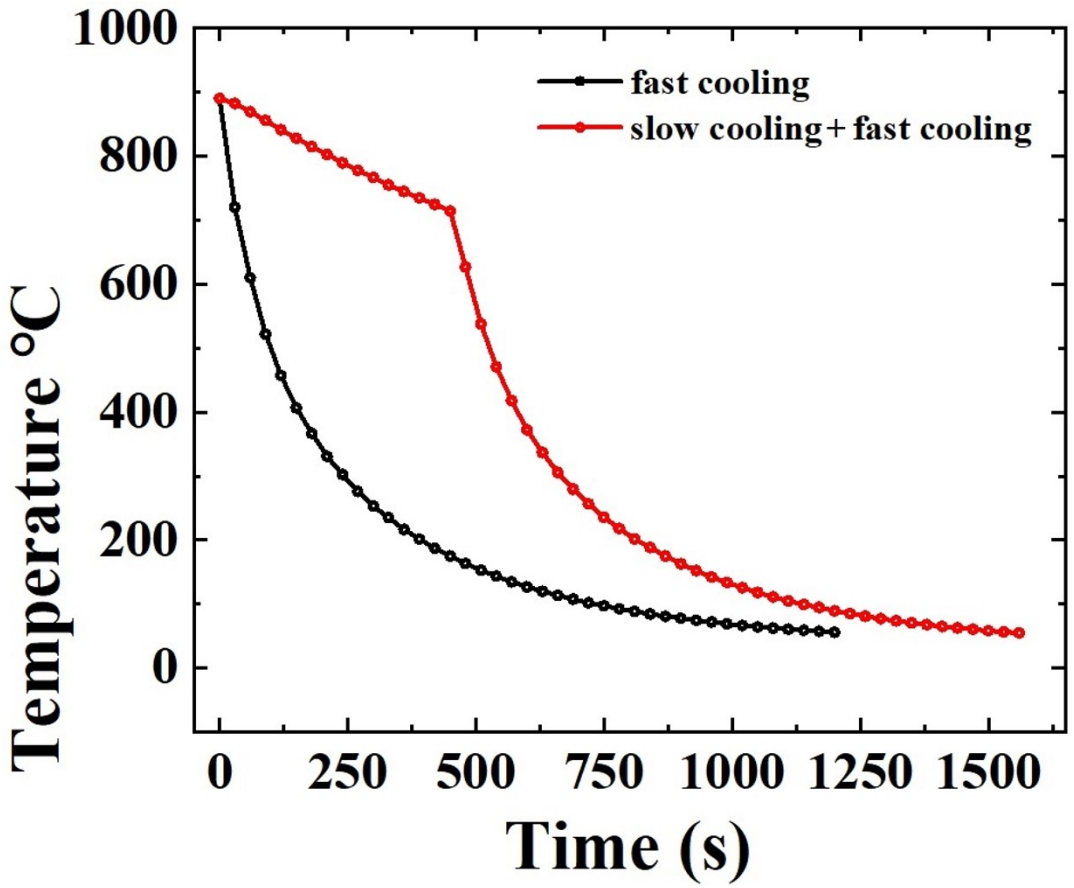

Figure S4: Cooling Profile, highlighting the importance of a combination of slow-cooling and fast-cooling approaches for the enhancement of the γ-Fe content (CNT-case, in absence of sulfur). Noticeably, the only fast cooling method (black) was employed in the CNO-fabrication experiments.

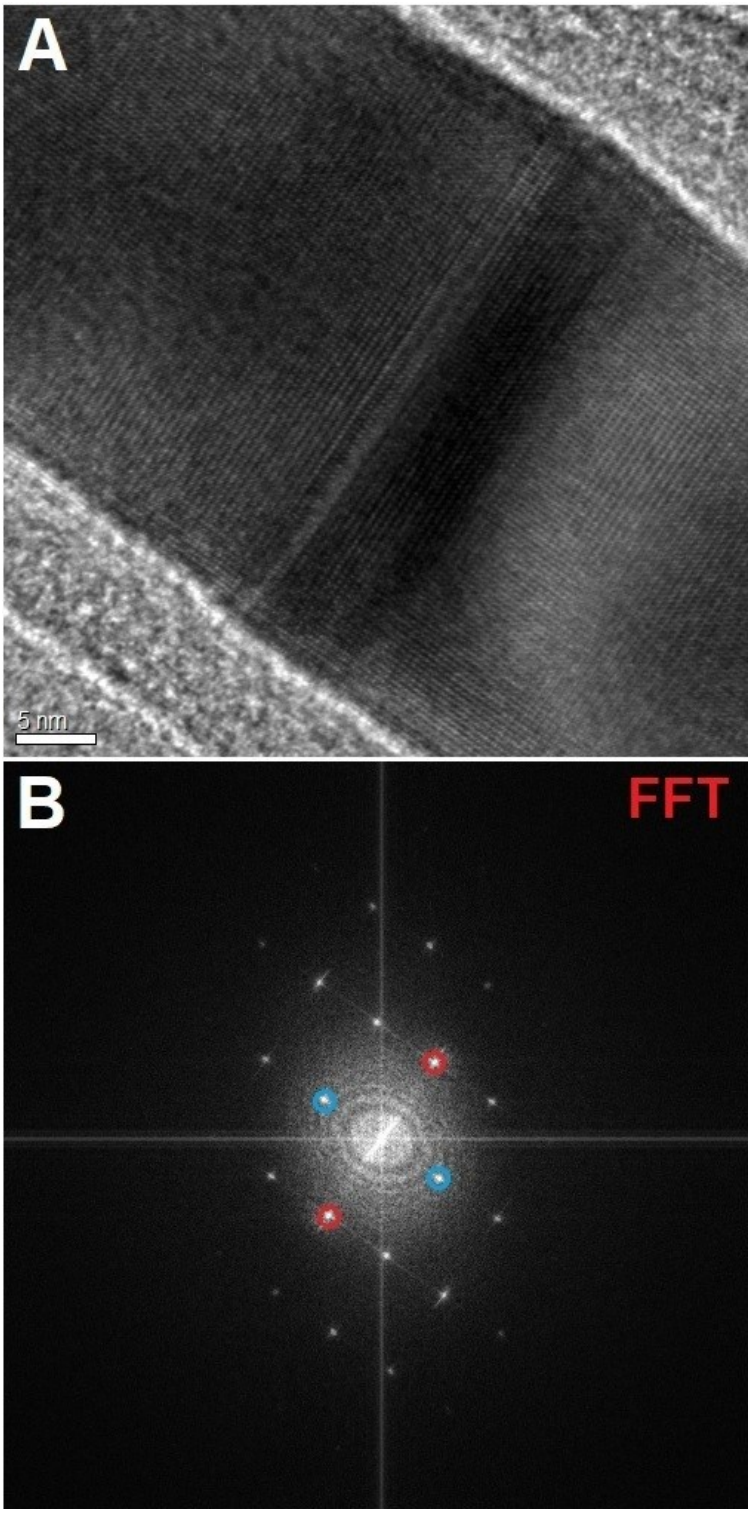

Figure S5: HRTEM and FFT analyses of the nanowire junction, encapsulated in a CNTs produced by pyrolysis of ferrocene/dichlorobenzene mixtures. The analysed area of the Fe_3C-nanowire, centred-on the step-junction is shown in A while the corresponding FFT analysis is presented in B. Interestingly, a single-crystalline-like arrangement is found within the regions centred-on and in proximity-of the junction, with the identification of preferred 100 (blue circles) and 011 reflections (red circles) of Fe_3C (space group Pnma) in B.

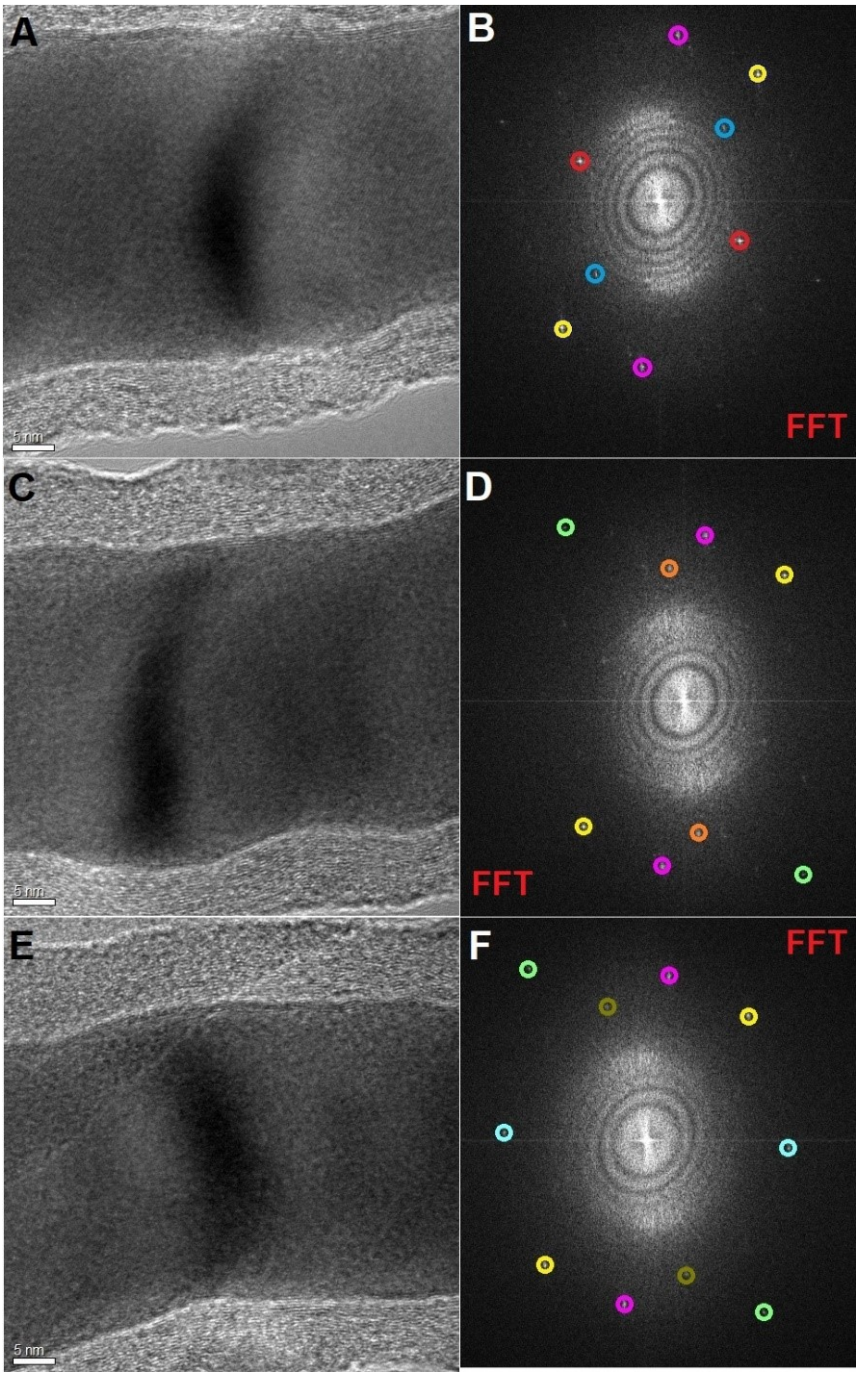

Figure S6: Unusual disorder-rich areas (A,C,E) distributed within the volume of an encapsulated nanowire, with characteristic faceted morphologies, indicative of a possible multi-grain arrangement. Interestingly, FFT analyses of these regions revealed the unusual coexistence of Fe_3C (CIF 1008725) and γ-Fe (CIF 1534888) within the faceted volume-regions of the nanowire (B, D, F). The observed diffraction spots correspond to the following lattice spacings. The yellow circles d~ 0.189 nm (131 reflection of Fe_3C), the blue circles 0.315 nm (111 reflection of Fe_3C), the pink circles 0.180 nm (200 reflection of γ-Fe), the red circles 0.338 nm (101 reflection of Fe_3C), the orange circles 0.229 nm (002 reflection of Fe_3C), the green circles 0.145 nm (103 reflection of Fe_3C), the dark yellow circles 0.217 nm (201 reflection of Fe_3C), the cyan circles 0.214 nm (211 reflection of Fe_3C).

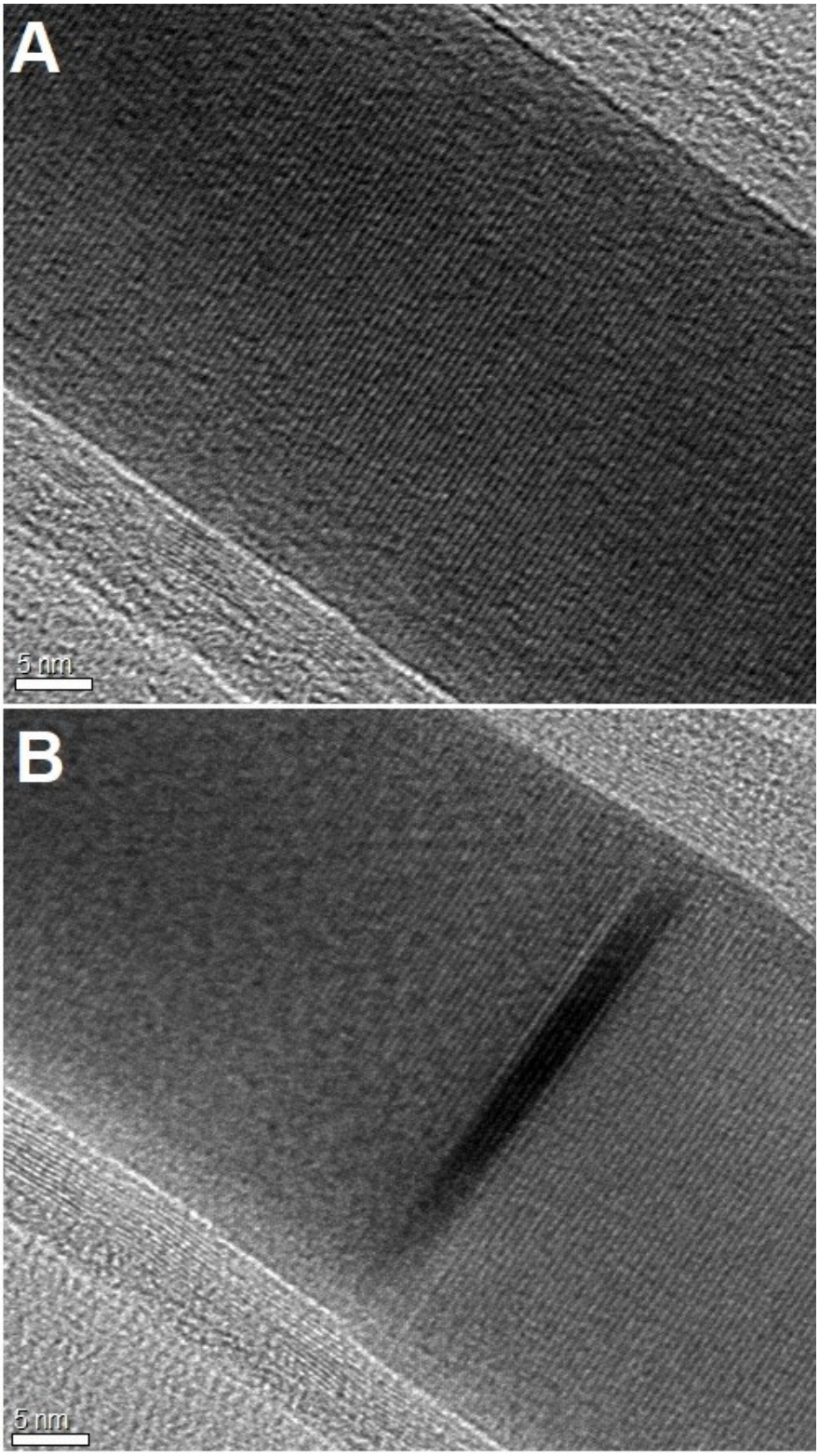

Figure S7: HRTEM micrographs evidencing 1) in A the presence of a single crystalline arrangement of the Fe_3C nanowire, with a preferred 100 orientation with respect to the CNT axis. 2) In B the observation of an unusual step-like junction, possibly arising from the rapid-cooling step.

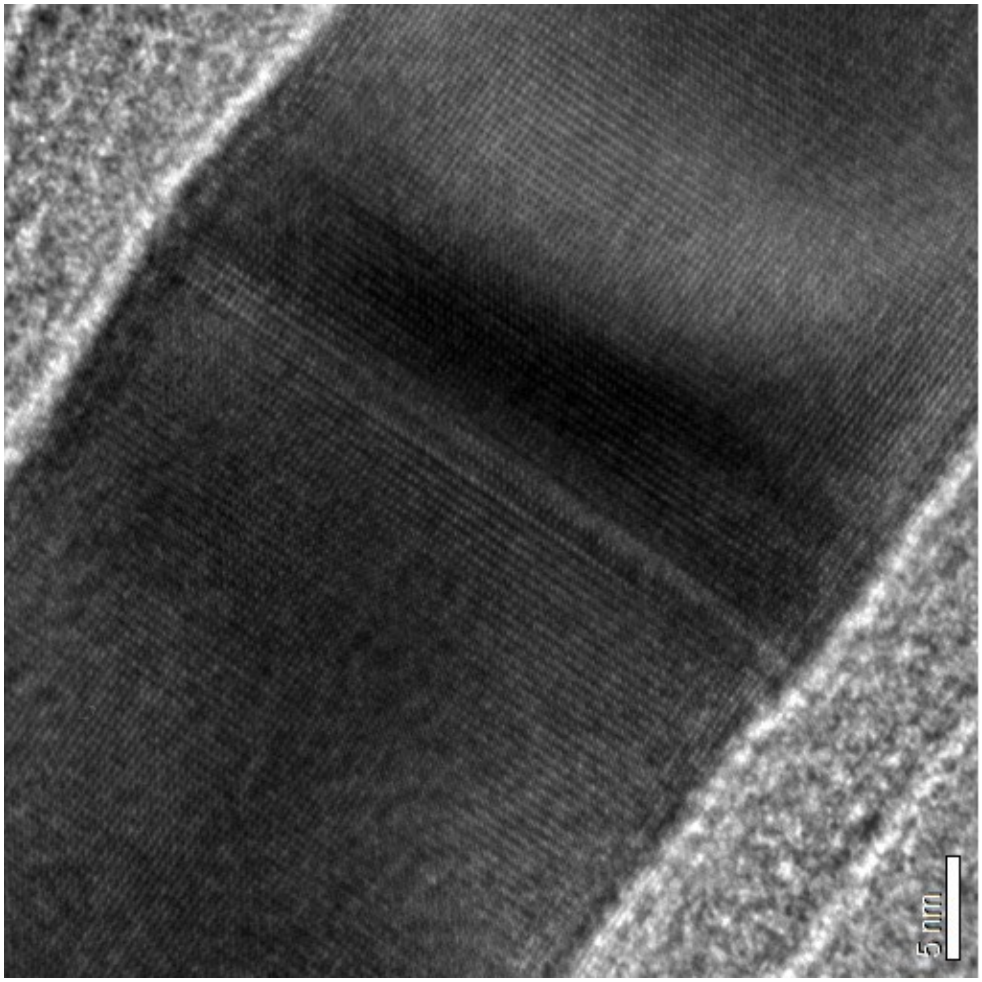

Figure S8: HRTEM micrograph evidencing another example of step-like magnetic junction nucleated in the encapsulated nanowire.

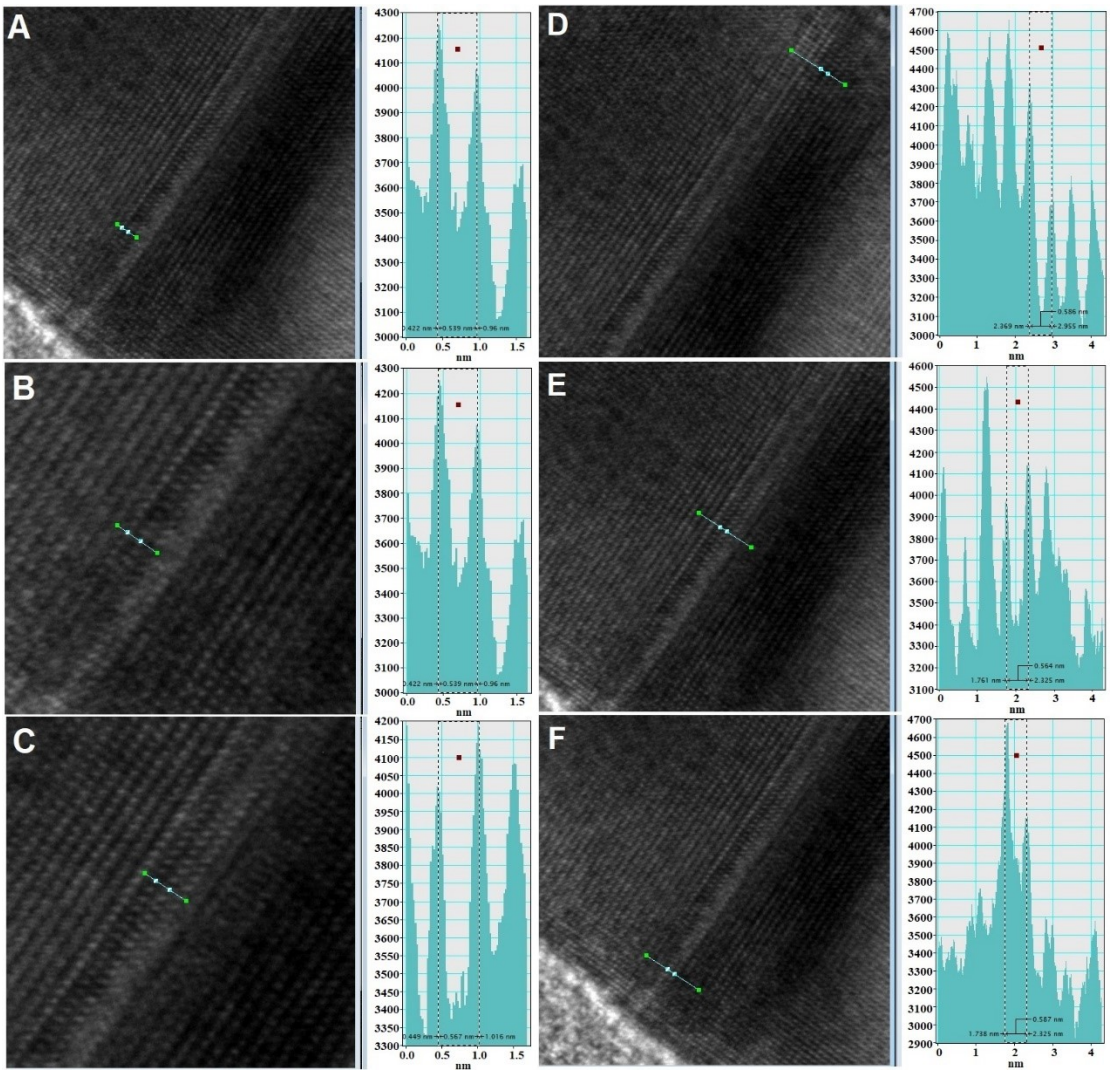

Figure S9: Additional HRTEM analyses performed on the lattice-regions centred on the junction (see A-F), by employing the profile-methodology in the software Digital Micrograph. An unusual enlargement of the 100 lattice-parameter of Fe_3C, with the d-value varying locally from 0.504 nm to 0.587 nm is found.

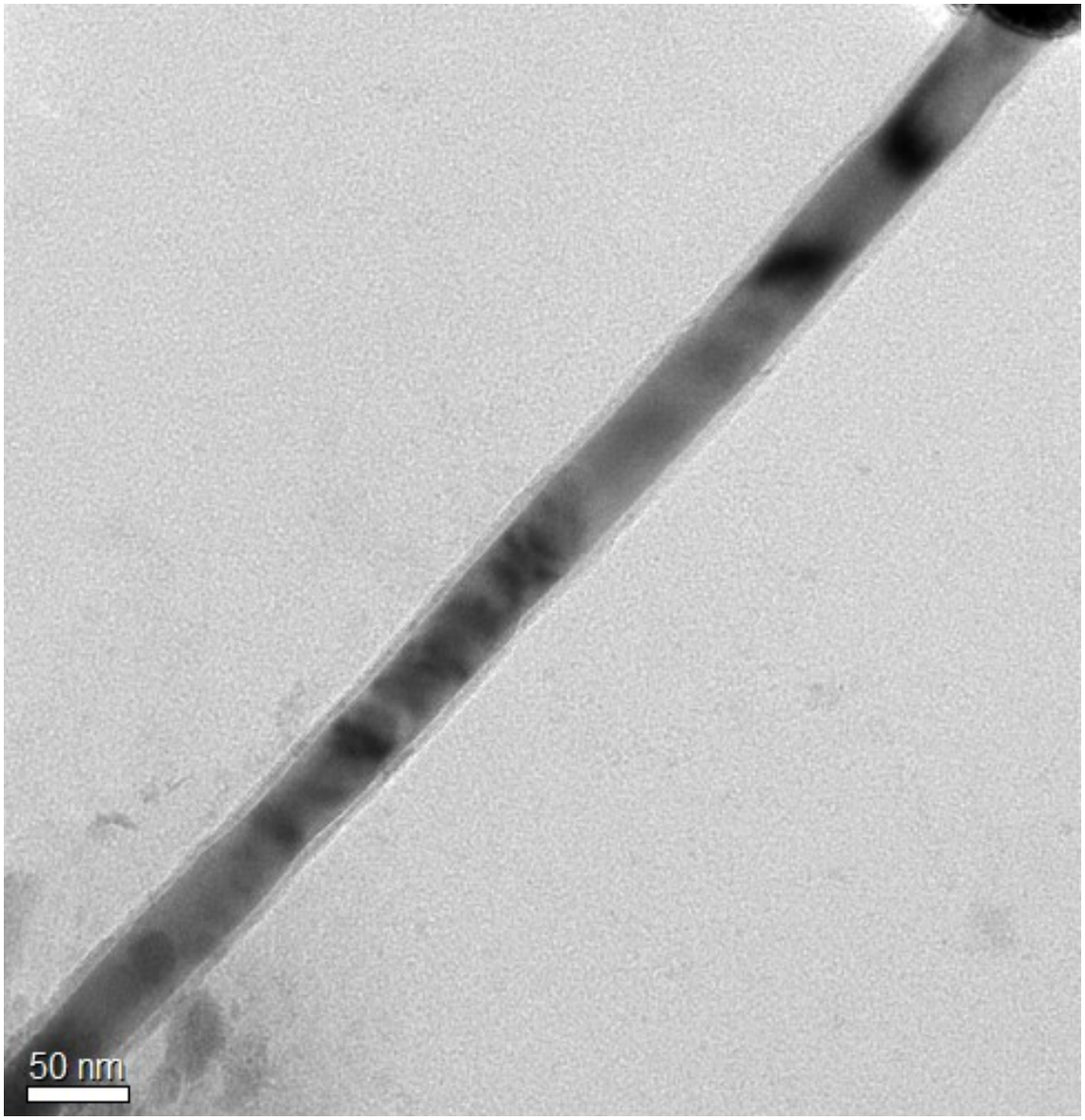

Fig.S10: Additional TEM micrograph exhibiting the high filling rate of the CNT-capillary.

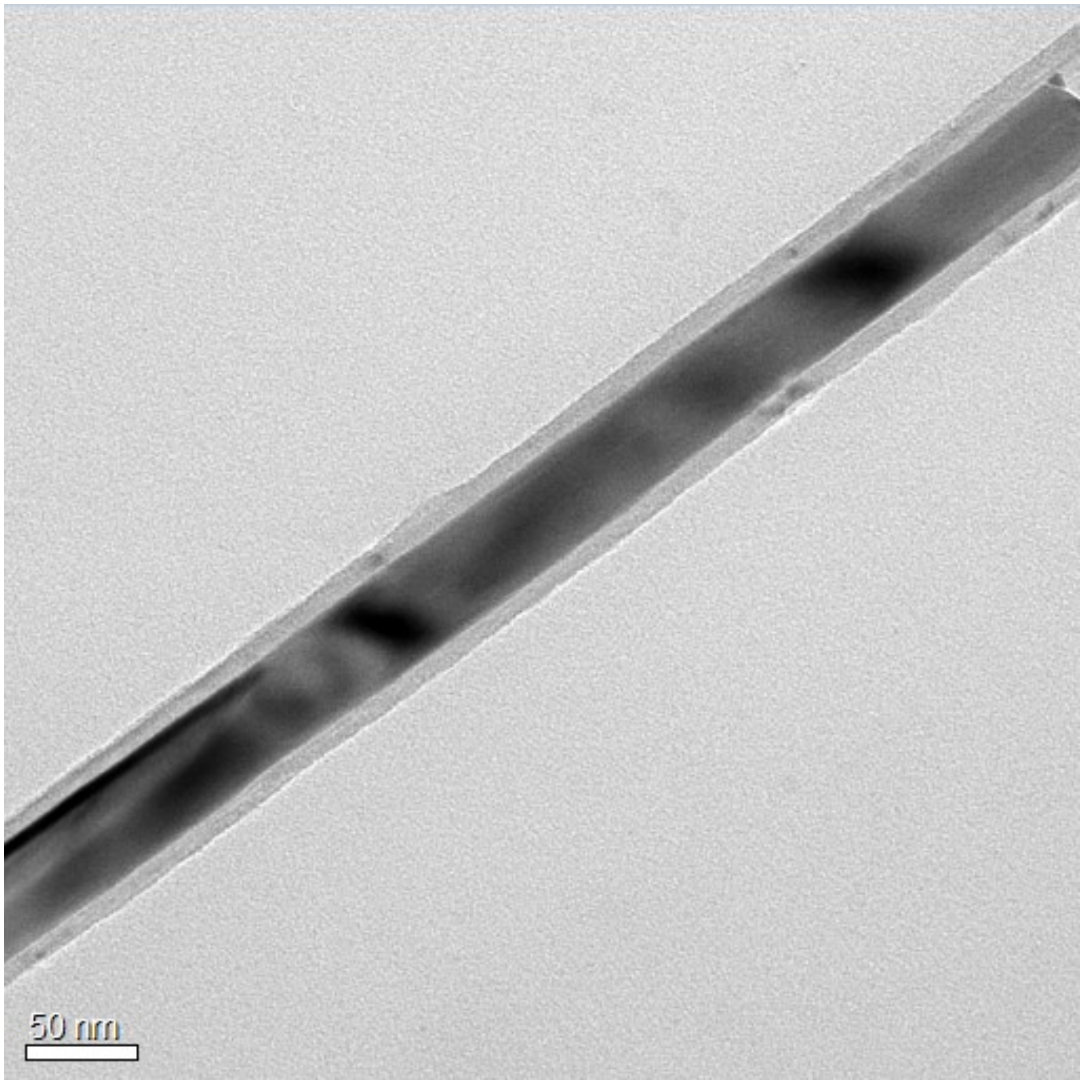

Fig.S11: TEM micrograph showing an additional example of the high filling rate of the CNT-capillary.

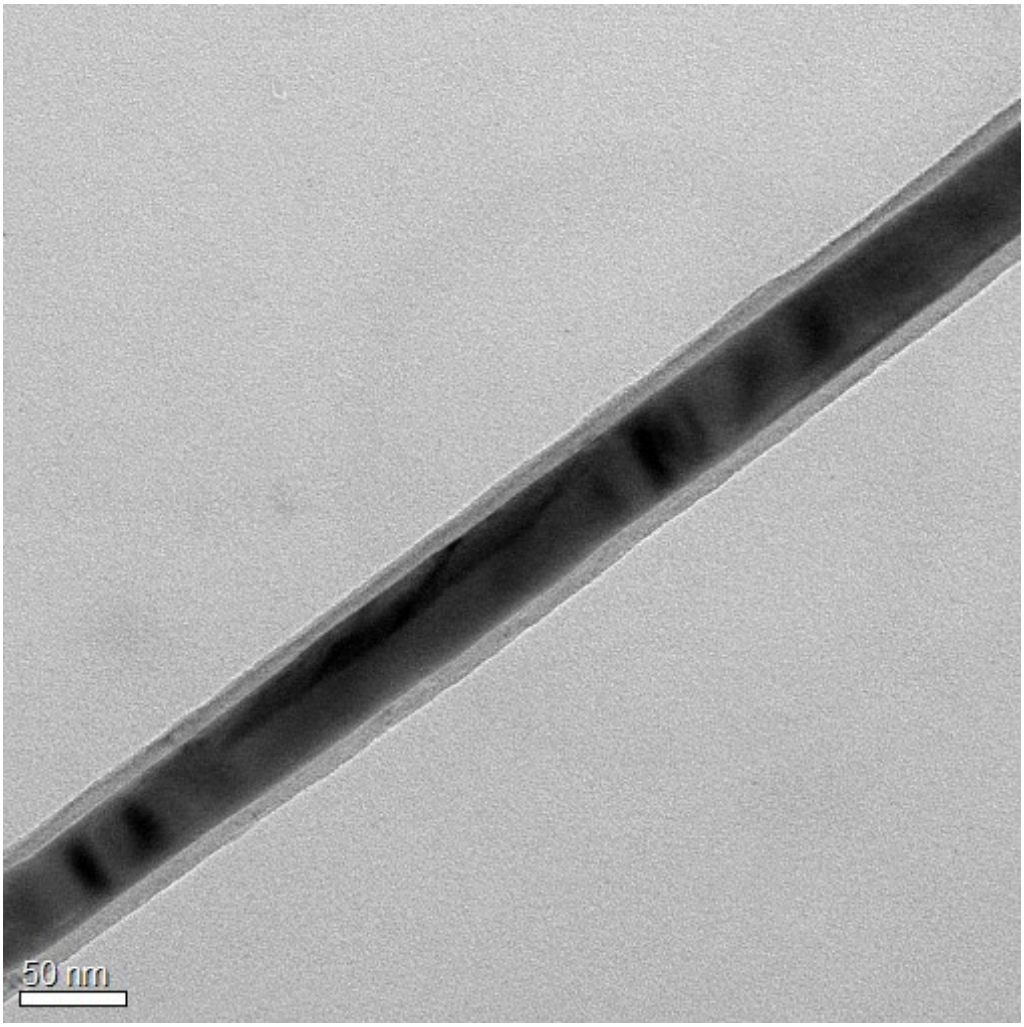

Fig.S12: TEM micrograph showing another example of the high filling rate of the CNT-capillary.

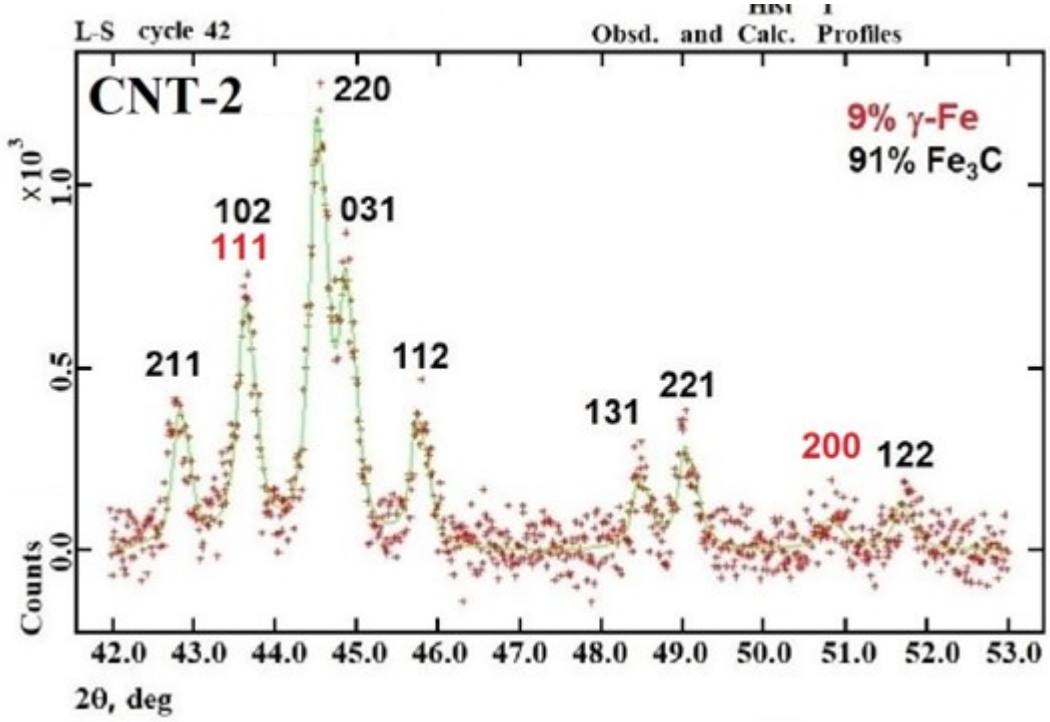

Figure S13: XRD diffractogram (red crosses) and Rietveld refinements (green line) acquired from a sample obtained with a combination of slow and fast cooling methods, in absence of sulfur (see Fig.S4 for cooling profiles).

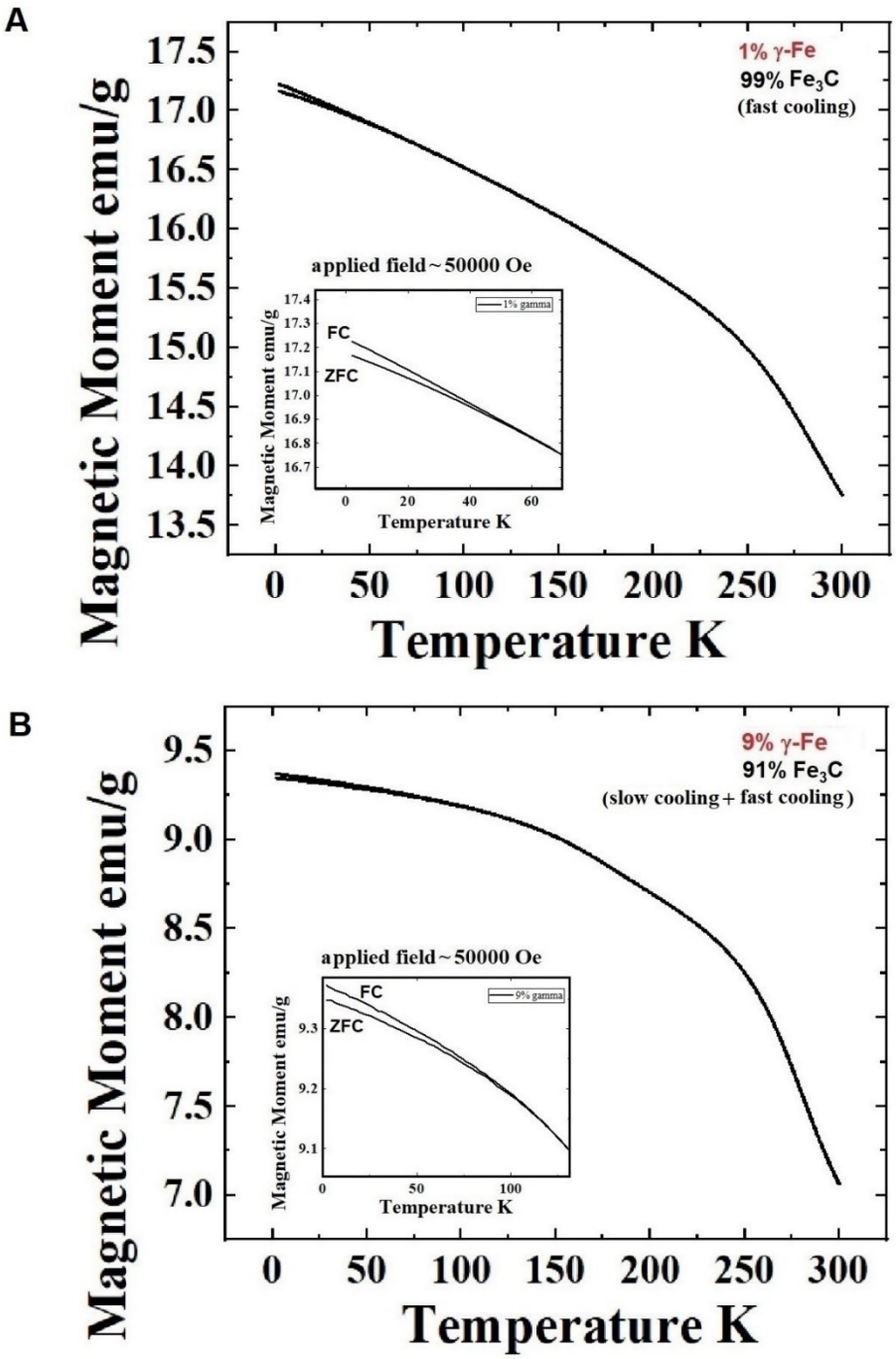

Figure S14: ZFC and FC magnetization curves acquired from two filled-CNT-samples produced by pyrolysis of ferrocene/dichlorobenzene mixtures, in absence of sulfur. The measurements were performed in the T-range from 2K to 300K at an applied field of 50000 Oe. The extremely low value of the magnetic moment appears to indicate a complex magnetic arrangement of the nanowires, strongly driven by the contributions arising from 1) the anisotropic behaviour (shape anisotropy) of the ferromagnetic Fe_3C phase (i.e. magnetic behaviour arising from interplay of shape and crystal anisotropies) and 2) the spatial phase distribution of the ferromagnetic γ-Fe phase, which is found to be located mostly in faceted regions of the nanowire.

Magnetic Properties of Fe_3C

Thanks to the significant magneto-crystalline anisotropy which originates from intrinsic spin orbit coupling contributions, single-crystalline iron-carbide can exhibit a ferromagnetic behaviour with large coercivities (~ 1000-2000 Oe) and saturation magnetizations (expected bulk saturation of ~ 169 emu/g). The encapsulation within the CNOs and/or CNTs allows for the stabilization of this phase and the protection from oxidation. The upper single domain limit for an approximately spherical Fe_3C single crystal can be calculated by considering the following equation (1) [Blundell S.].

$$r_{Fe_3C} < \frac{9\pi\sqrt{A(K_{sa} - K_{ma})}}{\mu_0 M_s^2} \qquad (1)$$

Where K_{sa} is the shape anisotropy energy density of an elongated Fe_3C ellipsoid of revolution (0.3×10^6J/m^3), K_{ma} is the magnetocrystalline anisotropy energy density of an elongated Fe_3C particle ($K_2 = 1.88 \times 10^5$J/m^3 and $K_1 = 0.394 \times 10^6$ J/m^3), M_s is the saturation magnetization (9.8×10^5A/m for Fe_3C) and A is the exchange stiffness constant that is 8.7×10^{-12} J/m for Fe_3C. The exchange stiffness constant can be written as shown in equation (2) [Supp.Ref.1-5]:

$$A = 2JS^2z/a \qquad (2)$$

Where J is the exchange integral, a is the nearest neighbour distance, z is the number of sites in the unit cell and S the spin [Supp.Ref.3].
In the case of Fe_3C an estimated critical single magnetic domain diameter of approximately ~ 42 nm would be expected.

Supplementary References:

[Supp Ref.1] Weissker U, Loffler M, Wolny F, Lutz M U, Scheerbaum N, Klingeler R, et al. Perpendicular magnetization of long iron carbide nanowires inside carbon nanotubes due to magnetocrystalline anisotropy. Journal of Applied Physics 2009; 106: 054909.

[Supp Ref.2] Lutz M U, Weissker U, Wolny F, Muller C, Loffler M, Muhl T, et al. Magnetic properties of α-Fe and Fe_3C nanowires. Journal of Physics: Conference Series 2010; 200: 072062.

[Supp Ref.3] Blundell S. Magnetism in Condensed Matter: Oxford Master Series in Condensed Matter Physics; 2001.

[Supp Ref.4] Sattler K D, Handbook of Nanophysics: Principles and Methods: CRC Press, Taylor and Francis group; 2011.

[Supp Ref.5] Getzlaff M. Fundamentals of Magnetism: Springer; 2003.